Petroleum and Coal

Review **Open Access**

CHARACTERIZATION OF SOURCE ROCKS AND DEPOSITIONAL ENVIRONMENT, AND HYDROCARBON GENERATION MODELLING OF THE CRETACEOUS HOIHO FORMATION, GREAT SOUTH BASIN, NEW ZEALAND

Liyana N. Osli, Mohamed R. Shalaby and Md. Aminul Islam*

Department of Geology, Faculty of Science, Universiti Brunei Darussalam, Jalan Tungku Link, BE 1410, Brunei Darussalam

Received December 12, 2017; Accepted February 10, 2018

Abstract

The Hoiho Formation in the Great South Basin (GSB) of New Zealand has been analysed for source rock characterization, hydrocarbon generation modelling, and interpretation of paleodepositional environment. Rock-Eval pyrolysis results from wells indicate the presence of excellent organic matter quality and quantity. The Hoiho Formation is dominantly of kerogen type II-III (oil and gas prone) and kerogen type III (gas prone). High values are also recorded for total organic carbon (TOC), hydrocarbon volume generated during pyrolysis (S_2) and hydrogen index (HI). Based on the maximum pyrolysis temperature and vitrinite reflectance values in Kawau-1A, Toroa-1 Tara-1 wells, it can be concluded that the Hoiho Formation is thermally mature only at the Central Graben of the basin, where these three wells are positioned at. Conversely, thermally immature source rock of the Hoiho Formation is recorded in the Hoiho-1C well. Important biomarkers and their derivatives, such as regular steranes, Pristane and Phytane confirm that Hoiho source rock was originally from a terrestrial source. One-dimensional basin modelling was applied to reconstruct the burial and thermal maturity histories of the formation. The top of oil window was reached at approximately 29 Ma, 53 Ma and 57 Ma at Kawau-1A, Toroa-1 and Tara-1 wells respectively.

Keywords: *Hoiho Formation; source rock characterization; burial history; Great South Basin; New Zealand*.

1. Introduction

The primary objective of this study is to describe and understand the source rock of the Hoiho Formation in the Great South Basin of New Zealand by focusing on the geochemical properties of the formation. This involves characterizing the source rock, studying the paleo-depositional environment, and producing hydrocarbon generation models. Despite not being commercially-productive, the Great South Basin hosts source rocks of high potential, including the Hoiho Formation. Because very little study has been done on this formation, it is therefore of a great interest to the authors of this paper to analyse this formation.

The Great South Basin (GSB) has a total area of 100,000 km^2 and is one of the largest basins in New Zealand (Fig.1), containing sediments of Late Cretaceous and Early Tertiary age that fill a series of grabens and half-grabens [1-5]. This deepwater basin was created in the Cretaceous and had experienced mild tectonism [2].

Extensive studies on the hydrocarbon potential of the Great South Basin have been conducted, such as those undertaken by Keuhnert [6], Gibbons and Jackson [7], Anderton *et al.* [8], Cook *et al.* [4], and Killops *et al.* [9]. This basin has been targeted for drilling, despite not having commercial hydrocarbon production [10]. Formations of interest for hydrocarbon exploration belong to Paleocene and Cretaceous, in which the lithology of source rocks are primarily coal and black marine shale [11].

One of the formations that displays a high potential as a source rock is the Hoiho Formation. This Formation is part of the Cretaceous Hoiho Group that represents the oldest sediments

and the main source of petroleum in the Great South Basin [4,12]. The Hoiho Formation contains syn-rift deposits consisting of organic rich clast-supported coaly sandstone.

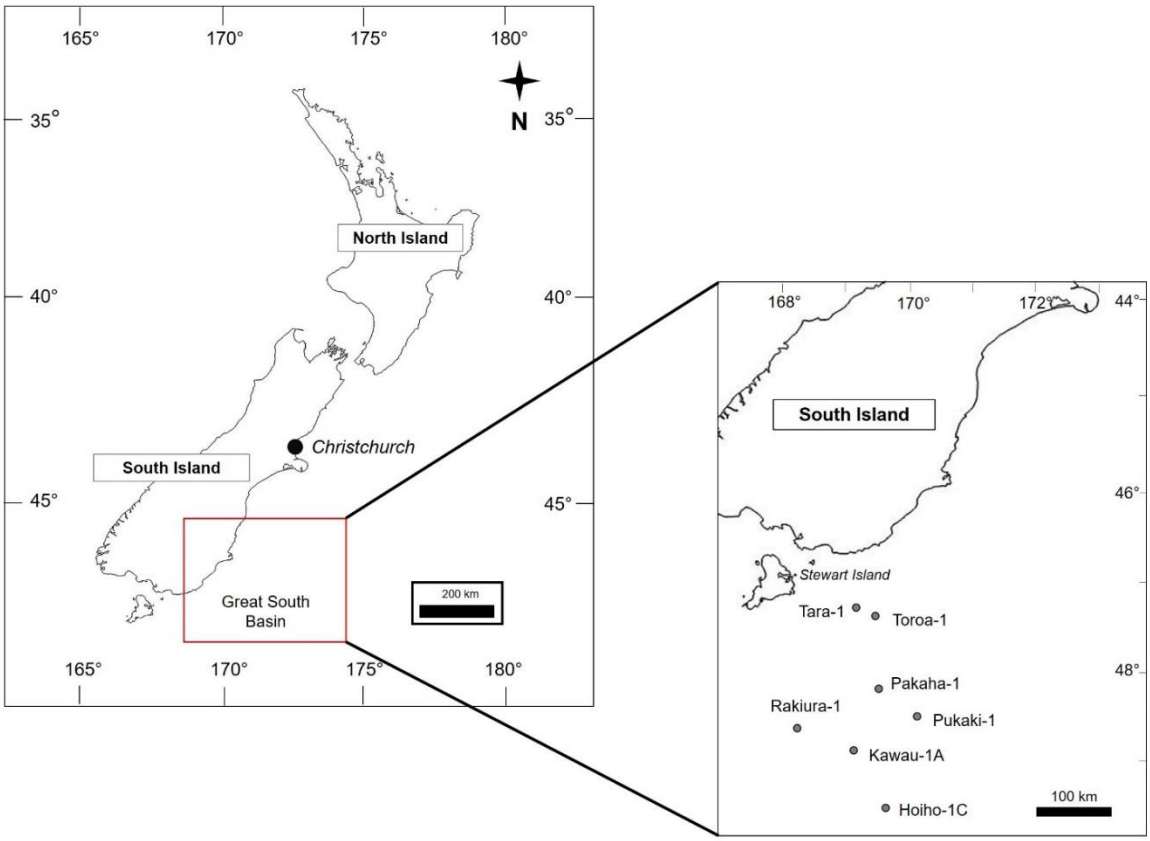

Figure 1. Map of New Zealand showing the location of the Great South Basin and the study area (*modified after Schiøler et. al.* [1])

Only four out of eight wells drilled in the Great South Basin suggested hydrocarbon generation [13]. Killops *et al.* [9] concluded that wells Kawau-1A, Toroa-1, and Pakaha-1 encountered gas condensate in Cretaceous sands. The Hoiho-1C well, drilled in 1978, encountered two source rocks but did not display any hydrocarbon show. Wells Tara-1 and Takapu-1 experienced several mechanical difficulties during drilling but later reported the absence of hydrocarbon, while the Tara-1 well showed gas at the top of the Cretaceous formations that were drilled. The Rakiura-1 well also failed to penetrate a good source rock, as the sands encountered were either of poor quality or immature. In the Great South Basin, the Pukaki-1 well is the most recent well drilled and recorded only minor methane [11]. Hydrocarbon quality in the wells of the Great South Basins has also been studied through Rock-Eval pyrolysis, in which the kerogen analysed was observed to be mainly humic in coaly sediments, affirming the dominance of gas condensate as encountered by the Kawau-1A, Toroa-1, Pakaha-1 and Tara-1 wells.

Rock-Eval pyrolysis for the Hoiho Formation is generally limited. Gibbons and Jackson [7] has stated that the predictions of oil potential in the Great South Basin are over-optimistic, as pyrolysis was performed on samples from the Kawau-1A and Toroa-1 wells only. Similarly, Rock-Eval data obtained from the Pukaki-1 and Rakiura-1 wells are also limited. Therefore, this paper aims to re-evaluate the Hoiho Formation as a source rock by using the data from four wells for Rock-Eval pyrolysis: the Hoiho-1C, Kawau-1A, Tara-1 and Toroa-1 wells (Fig. 2). Assessment of the Hoiho Formation also includes generating one-dimensional models to understand the formation's burial and thermal maturity histories and characterizing the paleo-depositional environment using biomarkers.

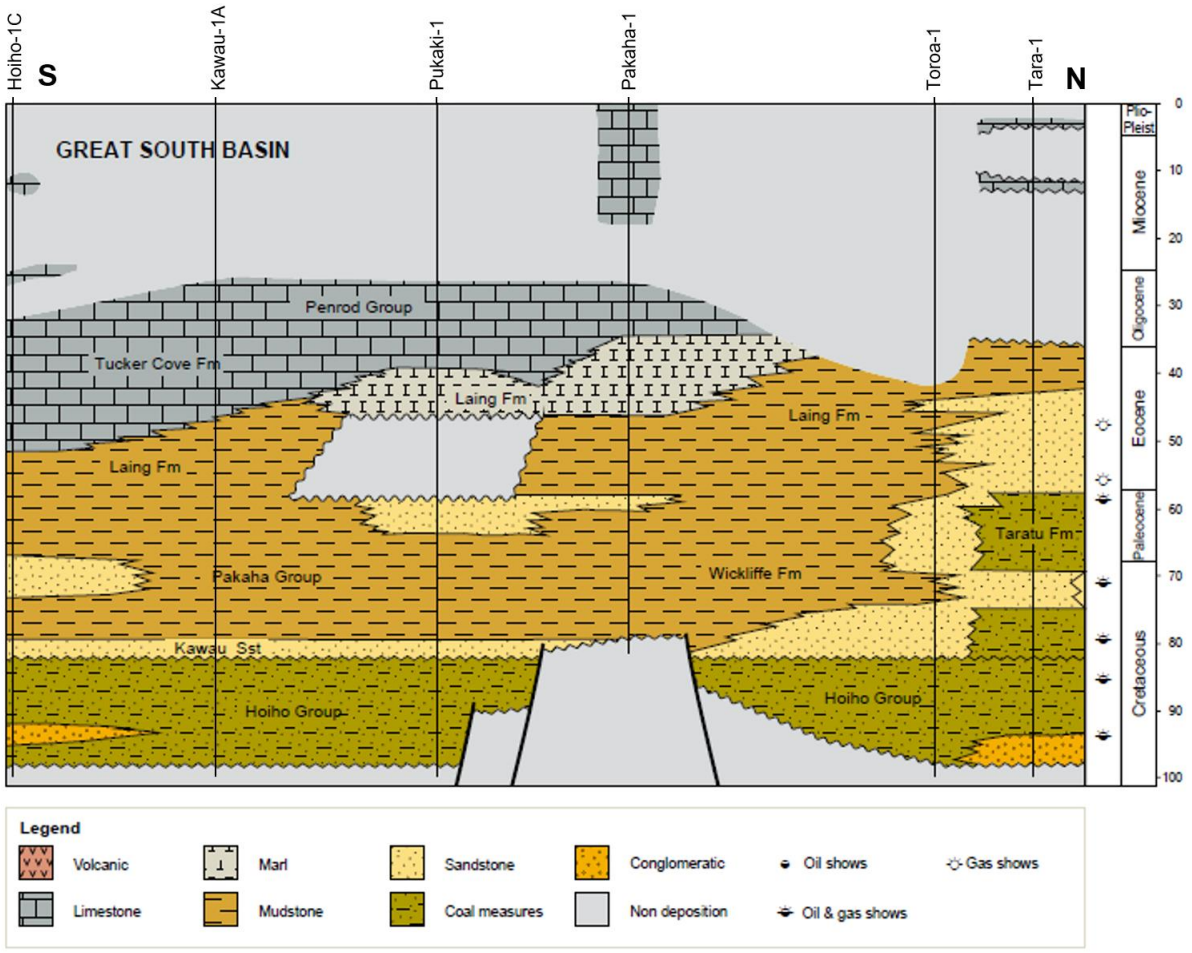

Figure 2. Stratigraphy of the Great South Basin (*Modified after New Zealand Petroleum and Minerals,* [10])

2. Geological settings and stratigraphy

The geological setting and stratigraphy of the Great South Basin has been studied by several authors, including McMillan and Wilson [14], Schiøler *et al*. [1] and Constable *et al.* [15]. The eastern part of New Zealand, where the Great South Basin is located, underwent more intense tectonic activities than the western margin**.** In the Cretaceous, there was a shift from a compressional to an extensional regime in the eastern New Zealand. Subduction of the Phoenix plate halted at approximately 105 -100 Ma from central New Zealand to the eastern tip of the Chatham Rise, and rifting initiated that eventually led to the separation of New Zealand from Gondwana [16]. This change caused widespread uplift and erosion creating a wide angular unconformity, called the Albian Unconformity, which extends throughout the whole of New Zealand.

It is also in the Cretaceous that the major tectonic episodes that initiated the formation of the Great South Basin began [10]. Initiation of rifting in the mid-Cretaceous created NW-SE trending grabens and half-grabens that underwent sedimentation [15]. Continuous sedimentation in the form of non-marine conglomerates, sandstone, mudstone, and coal from fluvial and lacustrine environments occurred during this period [10,15-16]. These rift-related sediments deposited in grabens and half-grabens make up the Hoiho Group (Fig. 2), which rests unconformably on the basement rocks of the Great South Basin. The basement rocks of the Great South Basin are primarily over thickened crust that generates high elevation blocks [17].

After this thick succession of fluvial and lacustrine sediments was deposited, accommodation space in the grabens began to decrease, allowing for marine influence. It is for this

reason that the Hoiho Group is thought to be overlain by delta plains that may host potential sand reservoirs and coaly source rocks [15]. As rifting waned, a basal transgressive sandstone called the Kawau Sandstone was deposited that hosts condensate gas in the Kawau-1A well [1,4] (Fig. 2). New Zealand completely separated from eastern Gondwana in the Late Cretaceous, which is marked by a marine transgression throughout New Zealand that peaked in the Oligocene [16]. This separation resulted in the formation of the Tasman Sea.

Rifting in the Great South Basin was followed by thermal subsidence that continued from Late Cretaceous to Paleogene [15]. Sediments deposited during this time include sandstone, greensand, and mudstone. Further subsidence of the basin initiated the deposition of carbonates and calcareous mudstone as the basin became a deep marine environment [9-10]

Throughout the Paleocene, there was a shift in the shoreline to the west [9]. In the western margin of the basin, a prograding delta began to form during the period of thermal subsidence. Upon the final opening of the Solander and Emerald sub-basins in approximately 45 Ma, supply of sediment to the delta terminated and transgressive sedimentation began (Fig. 2). In the Oligocene-Miocene, the western margin of the Great South Basin was affected by plate tectonics, as movement along the Alpine Fault was initiated [15,18].

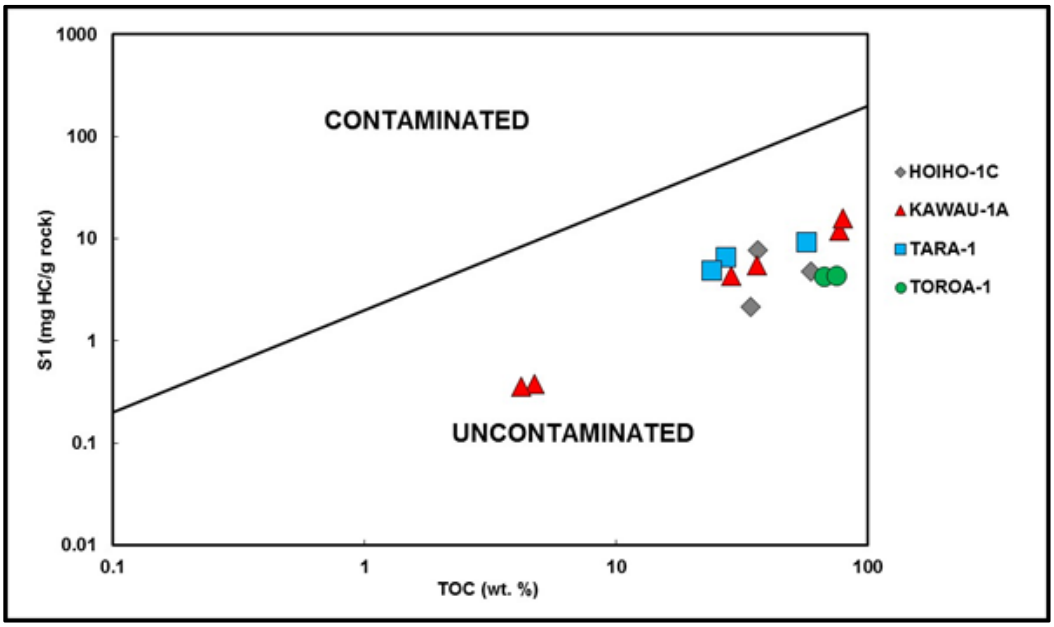

Figure 3. A cross-plot of S_1 versus TOC to indicate the origin of hydrocarbon in the Hoiho Formation *(Fakhri et al. [54])*

Compressional stresses from mountain-building along the Alpine Fault became amplified, and the western margin of the basin was folded into anticlines and synclines, creating uplift in this part of New Zealand [10]. A thick prograding marine sequence is found in this part of the basin and trends north east [1,16]. After the Miocene, thick successions illustrating marine progression were deposited in the western Great South Basin. In the eastern part of the basin, there was an accumulation of Neogene age pelagic sediments [9].

3. Data and methods

All data sets were provided and permitted for publishing by the Ministry of Business, Innovation and Employment (MBIE) of New Zealand together with GNS Science. Twenty-seven drill cutting samples belonging to the Hoiho Formation from the Hoiho-1C, Kawau-1A, Tara-1 and Toroa-1 wells were used to Rock-Eval pyrolysis.

Rock-Eval 2 and 6 are used in this study with the aim of investigating the hydrocarbon potential, maturity, and type of organic matter [19-20]. Pyrolysis results include the volume of free hydrocarbon or bitumen available in the source rock before pyrolysis (S_1), the volume of

hydrocarbon generated during pyrolysis (S_2), amount of carbon dioxide emitted (S_3), Total organic carbon (TOC), vitrinite reflectance (R_o), and maximum pyrolysis temperature (T_{max}). The Hydrogen Index (HI) and Oxygen Index (OI) were calculated using the given data [20-21]. Other calculations from the pyrolysis results applied in this study include the Production Yield ($PY=S_1 + S_2$) and the Production Index ($PI=S_1/S_1+S_2$)

The paleodepositional environment of the Hoiho source rock is evaluated through the application of biomarker data from the Hoiho-1C and Kawau-1A wells. Biomarker data and important derivations were interpreted according to studies done by Rodriguez and Philp [22], Abdullah *et al.* [23] and Ayinla *et al.* [24]. Studying the environment where the Hoiho source rock was deposited provides a background understanding and confirmation of the kerogen types generated in the Hoiho Formation. In addition to the paleodepositional environment, using biomarkers and their derivations such as the pristane/phytane ratio, isoprenoid/n-alkanes ratio, concentration of regular steranes (C_{27}, C_{28} and C_{29}), and the carbon preference index (CPI) can be used to determine the quality and thermal maturity of the source rock.

In assessing the Hoiho source rock's burial and thermal maturity histories, the utilization of the PetroMod software is necessary. Relevant input parameters for one-dimensional basin modelling are derived from completion reports, composite logs, and the well card summary for all wells in the study. These parameters include the formations detected in each well, formation thickness (metres), formation age (Ma), measured borehole temperature (°C), and measured vitrinite reflectance (%R_o). It is also important to identify individual petroleum system elements for every stratigraphic sequence detected in each well. For the studied source rock, other geochemical parameters such as TOC and HI are required.

Calibrating measured and calculated values for borehole temperature and vitrinite reflectance was performed to examine the quality of data used in this study. Prior to calibration, every borehole temperature extracted from composite logs must be corrected to eliminate inaccuracies attributed to the lack of equilibrium between the formation temperatures and those of the drilling mud. In this study, borehole temperature correction was done based on the studies by Waples and Ramly [25], Waples and Ramly [26], Peters and Nelson [27] and Bullard [28]. Modelled vitrinite reflectance values are calculated using the EASY%R_o model [29]. The 1-D modelling of the formation is expected to constrain the burial history, thermal maturity history, and timing of hydrocarbon generation in the Hoiho Formation. Only the Kawau-1A, Toroa-1 and Tara-1 wells were used for modelling.

4. Results and discussion

4.1. TOC and rock-eval pyrolysis results

Based on this study, the Hoiho Formation has S_1 values that range from 0.36 to 15.76 mg HC/g. T_{max} values are recorded to be between 421°C to 472°C, which provide S_2 values for the source rocks. All wells generate good to excellent S_2 values, ranging from 5.95 to 174.79 mg HC/g rock, and S_3 values are documented ranging from 0.44 to 15.15 mg CO_2/g rock. Source rocks contain TOC values range from 4.21% to 77.03%, making the Hoiho Formation a promising potential source rock with excellent quantity of organic matter, based on the TOC classification introduced by Peters [20]. PI values for source rocks range from 0.04 to 0.11. Derived OI values of 2.71 to 25.53 mg CO2/g TOC were recorded in this formation and calculated HI values range from 9.52 to 293.3 mg HC/g TOC.

PY values are between 6.33 and 190.6 mg HC/g TOC and vitrinite reflectance (% R_o) values range from 0.36 to 1.42% R_o. The results of rock-eval pyrolysis and other parameters calculated are summarized in Table 1.

The S_1 versus TOC plot is used to investigate the origin of the hydrocarbon found in the source rocks (Fig. 3). In this cross-plot, it is found that the hydrocarbon from all wells is uncontaminated or autochthonous, which means that the hydrocarbon hosted by the source rocks did not migrated from elsewhere. PY can be plotted with TOC (Fig. 4) to estimate the hydrocarbon generation potential [30-34]. Figure 4 demonstrates the good to excellent capability of the Hoiho Formation to generate hydrocarbon.

Table 1 Rock-eval pyrolysis results used in this study

Well name	Depth (m)	Lithology	S_1	S_2	S_3	TOC	OI	HI	PI	S_2/S_3	S_1+S_2=PY	T_{max}
Hoiho-1C	1975	Coal	7.8	107.3	8.25	36.57	22.6	293.3	0.07	13.0	115.1	421
	2286	Coal	4.78	93.9	15.15	59.35	25.5	158.3	0.05	6.20	98.7	423
	2286	Shaly coal	2.17	48.2	7.63	34.37	22.2	140.3	0.04	6.32	50.4	423
Kawau-1A	3299	Coal	11.92	168.6	3.12	77.03	4.05	218.8	0.07	54.0	180.5	443
	3299	Shaly coal	4.35	64.9	1.59	28.71	5.54	226.2	0.06	40.8	69.3	441
	3299	Mudstone	0.38	5.95	0.44	4.73	9.30	125.8	0.06	13.5	6.33	437
	3303	Coal	15.76	174.8	3	79.8	3.76	219.0	0.08	58.3	190.6	446
	3303	Shaly coal	5.51	78.2	1.61	36.11	4.46	216.4	0.07	48.5	83.7	442
	3303	Mudstone	0.36	4.95	0.44	4.21	10.5	117.6	0.07	11.3	5.31	439
Tara-1	4310	Mudstone	6.6	52.5	3.3	27.2	12.1	193.0	0.11	15.9	59.1	456
	4365	Coal	9.3	89.6	9.5	57	16.7	157.2	0.09	9.43	98.9	456
	4365	Mudstone	4.9	47.3	2.3	24	9.58	197.1	0.09	20.6	52.2	458
Toroa-1	4327	Coal	4.23	86.0	2.22	67.31	3.30	127.8	0.05	38.7	90.2	468
	4494	Coal	4.38	83.3	2.04	75.15	2.71	110.8	0.05	40.8	87.7	472

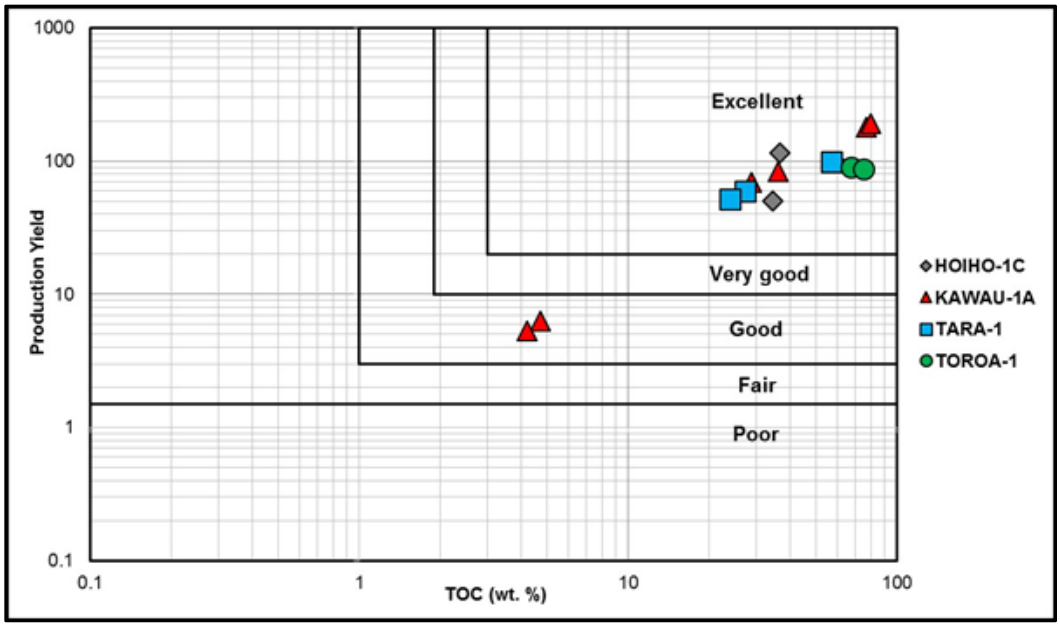

Figure 4. A cross-plot of PY versus TOC to demonstrate the generating potential of the Hoiho Formation

4.2. Types of organic matter

Accurate identification of genetic organic matter type is required to determine the characteristics of the hydrocarbon discharged and this is achievable using various pyrolysis results.

A S_2-TOC cross plot (Fig. 5) is used to investigate the hydrocarbon quality and quantity. The result suggests excellent organic matter quantity based on the TOC concentration in the

source rock, and a good to excellent hydrocarbon quality. Plotting S_2 versus TOC as done by Langford and Blanc-Valleron [35] (Fig. 6) also shows that most samples contain a mixture of kerogen type II-III and kerogen type III, although the organic matter in Toroa-1 shows only gas prone source rock of kerogen type III.

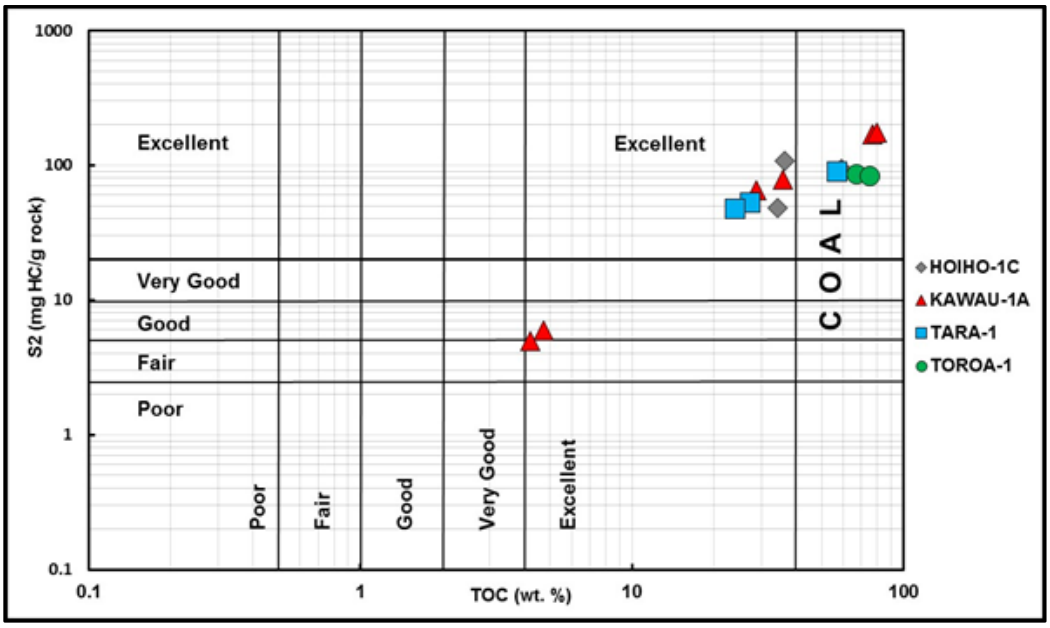

Figure 5. A cross-plot of S_2 versus TOC to demonstrate the quality and quantity of hydrocarbon *(Espitalié et al. [36])*

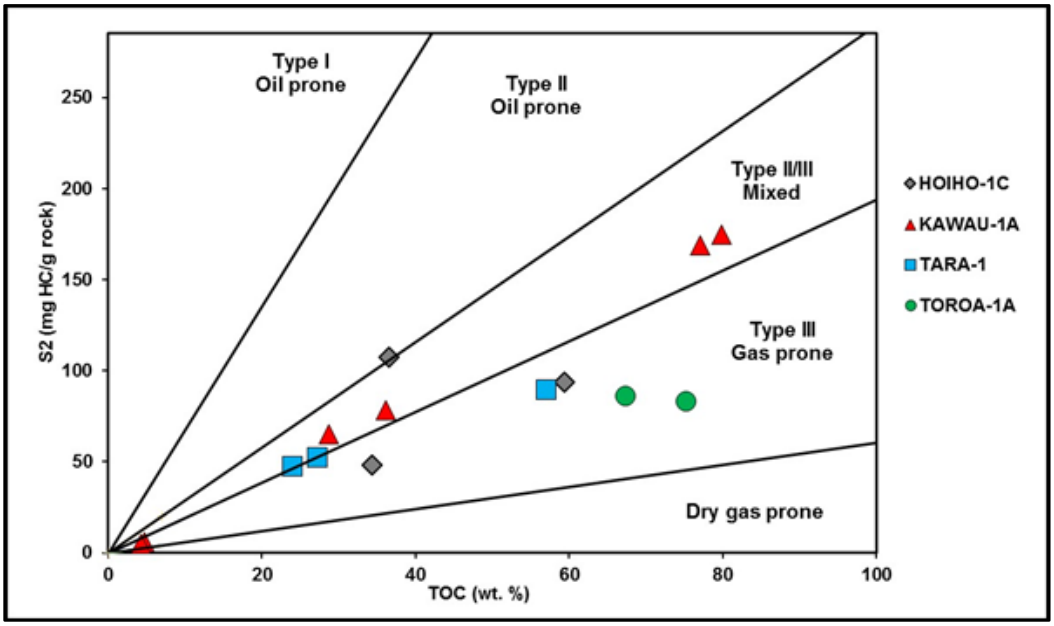

Figure 6. A cross-plot of S_2 versus TOC to identify the type of hydrocarbon produced from every wells *(Langford and Blanc-Valleron [35])*

The Van Krevelen diagram (Fig. 7) shows the relationship between HI (mg HC/g TOC) and OI (mg CO2/g TOC) [19,36-38]. HI and OI are defined through the formulae (HI = S_2/TOC x 100) and (OI = S_3/TOC x 100) respectively. These parameters consider the amount of hydrogen and oxygen with respect to the hydrocarbon produced by the source rock [20]. The modified Van Krevelen diagram (Fig. 7) shows HI values for the study ranging from 140.26 to 293.3

mg HC/g TOC. The outcome of the correlation between these values indicates the presence of kerogen II-III (oil and gas prone) and kerogen type III (gas prone) [38]. This result provides a confirmation of the results from the S_2-TOC cross plot in Figure 6.

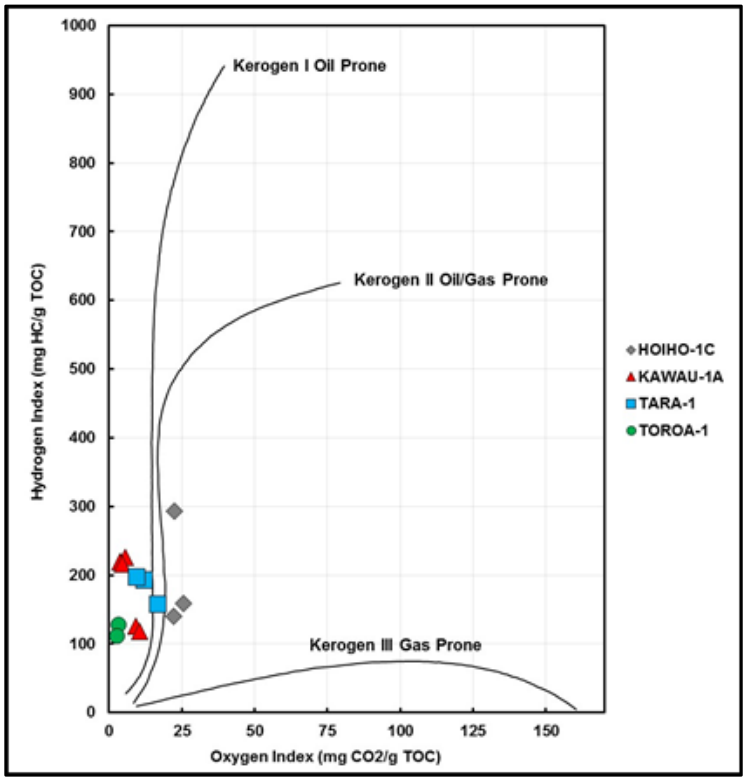

Figure 7. A cross-plot of HI versus OI in the modified Van Krevelen diagram shows the type of kerogen available in the source rock *(Espitalié et al. [36])*

4.3. Thermal maturity and hydrocarbon generation potential

Thermal maturity is an important factor in source rock evaluation. Indicators of thermal maturity include T_{max}, R_o, and PI, which will be correlated with the other pyrolysis results to demonstrate the evolution of Hoiho source rock maturity.

By definition, T_{max} is the pyrolysis temperature which produces the maximum amount of hydrocarbon from the thermal degradation of kerogen [39], and an increase in T_{max} values indicates increasing organic matter evolution [21,40]. A classification introduced by Peters [20] relating to hydrocarbon type and T_{max} marks the temperature range of 430°C-445°C as the beginning of the mature oil window. At 470°C, oil is no longer produced and gas generation is initiated.

A cross-plot between T_{max} and HI (Fig. 8) shows that the organic matter in Hoiho-1C well is thermally immature. All points belonging to Kawau-1A well are located within the mature oil window, with T_{max} values ranging from 437°C to 446°C. Tara-1 and Toroa-1 contain points that lie at the early and late ends of the condensate wet gas window respectively, making the organic matter in Toroa-1 almost thermally over-mature with a T_{max} of 468°C and 472°C. Figure 8 also shows good agreement with Figures 6 and 7, confirming the kerogen type present in the Hoiho Formation as kerogen type II-III and kerogen type III.

Vitrinite reflectance is the proportion of normal incident light reflected by a plane polished surface of vitrinite, which alters according to the level of maturation [41]. Similar to T_{max}, more mature samples reflect higher % R_o values, therefore an increase in % R_o is expected with increasing depth [42]. However, these values are only available if the samples originate from a continental source, therefore only coal samples in this study were tested for vitrinite reflectance [43]. The cross-plot of T_{max} and % R_o can be used to further understand the thermal

maturity of the source rock, as displayed in Figure 9 [44]. This figure shows a positive correlation between both indices, and indicates thermally immature source rock in Hoiho-1C, mature source rocks in Kawau-1A and Tara-1, an almost over-mature organic matter in Toroa-1. Values for vitrinite reflectance together with their respective well names are summarized in Table 2.

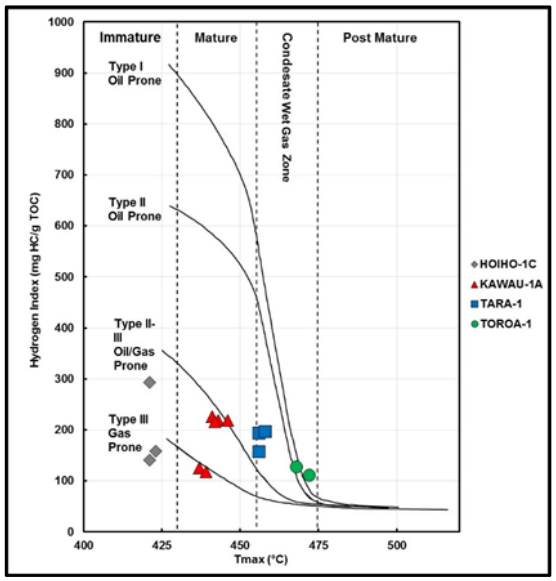

Figure 8. A cross-plot of HI versus T_{max} to indicate source rock thermal maturity

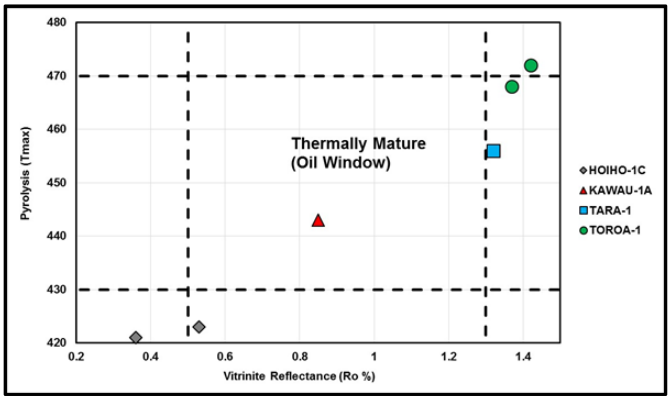

Figure 9. A cross-plot of T_{max} versus R_o to indicate source rock thermal maturity

Table 2. Vitrinite reflectance values used in this study

Well name	Depth (m)	% Ro	Well name	Depth (m)	% Ro
Tara-1	944.8	0.34	Hoiho-1C	1938.2	0.36
	1188.7	0.39	Kawau-1A	2621.2	0.62
	1341.1	0.35		3169.8	0.72
	1584.9	0.38		3291.2	0.85
	1676.3	0.37	Toroa-1	4327	1.37
	1859.2	0.37		4327.9	1.12
	2011.6	0.46		4358.4	1.17
	2438.3	0.45		4388.9	1.19
	2468.8	0.53		4419.4	1.2
	2834.5	0.58		4449.9	1.2
	3047.9	0.6		4480.3	1.22
	3169.8	0.65		4494	1.42
	3169.8	0.7		4510.8	1.24
	3474.6	0.7		4541.3	1.26
	3840.3	0.83		4551.4	1.27
	4145.1	0.89			
	4365				
	1.32				

PI can be used to determine thermal maturity [20,30-34]. PI is the proportion of the amount of the free hydrocarbons already generated to the total amount of hydrocarbon that the organic matter is capable of generating [19,38]. The plot of PI versus T_{max} (Fig. 10) shows that the organic matter for the Hoiho Formation in the four wells grade from immature to over-mature with values ranging from 0.04 to 0.11. This cross-plot is in good agreement with Figure 9, demonstrating the presence of organic matter in several thermal maturity stages for Hoiho source rocks.

On the other hand, the Toroa-1 well has a lower PI value (0.05). The data indicating over maturity in this well, T_{max} (468-472°C) and vitrinite reflectance R_o% (1.37-1.42%), are inconsistent with the PI value. The reason for this is well described by Abdullah *et al.* [56]; it can be due to different lithology, nature of kerogen, or even the preservation condition of organic matter.

A cross-plot of TOC versus depth from different wells (Fig. 11) shows that majority of the Hoiho Formation contains an excellent hydrocarbon quantity regardless of the formation's depth. However, depth affects the organic matter quality and thermal maturity (Figs. 12-13).

The Hoiho Formation is encountered at a shallow depth in Hoiho-1C well, at a depth of 1966 to 2286 metres, compared to the other wells. Conversely, the formation is found to be over-mature in Toroa-1 well, as the condensate gas window is already reached at greater depths with high T_{max} (Figs. 12-13).

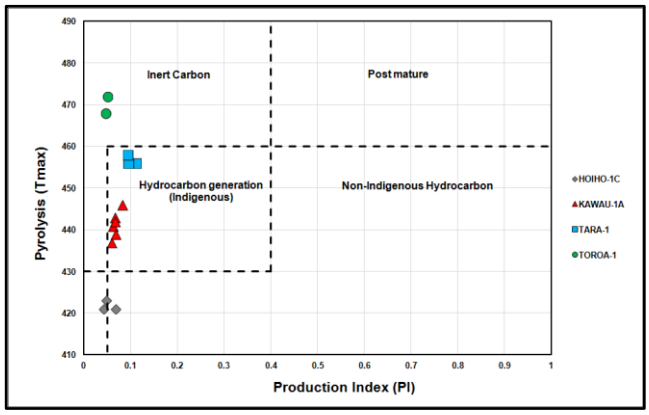

Figure 10. A cross-plot of T_{max} versus PI to identify source rock maturity

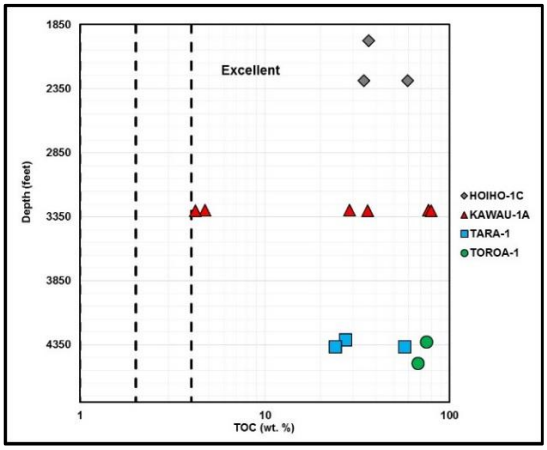

Figure 11. Cross-plot of TOC versus depth to demonstrate the distribution of the parameter with increasing depth *(Shalaby et al.* [33] *)*

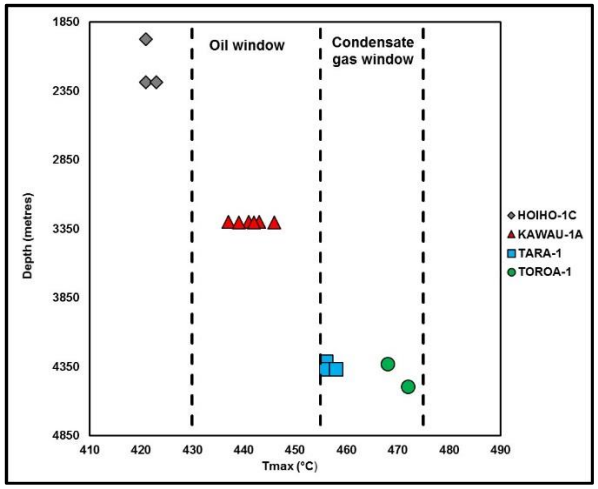

Figure 12. Cross-plot of T_{max} versus depth to demonstrate the distribution of the parameter with increasing depth *(Shalaby et al.* [33]*)*

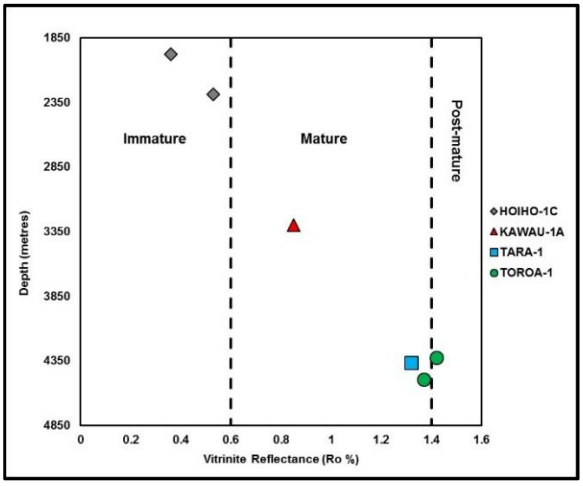

Figure 13. Cross-plot of R_o versus depth to demonstrate the distribution of the parameter with increasing depth *(Shalaby et al.* [33]

Difference in thermal maturity recorded in all four wells is attributed to the positions of these wells in the Great South Basin. Thermal maturation of the Hoiho Formation encountered in Kawau-1A, Toroa-1 and Tara-1 wells is resulted from to the positions of these wells at the Central Graben of the Great South Basin, where sediments are the thickest.

Good homogeneity is shown for all four wells, whereby a gradation of maturity-measuring parameters, such as T_{max} and % R_o, is recorded as the Hoiho Formation is encountered at varying depths across the wells.

4.4. Paleodepositional environment

Biomarkers are one of the important means to assess a source rock's paleodepositional environment. They are ubiquitous in nature and can be distinct when evaluating a specific source rock depositional facies [45]. Biomarkers utilized for evaluating source rocks are derived from organic compounds of previous living organisms [46]. Different biomarker parameters and their derivations can be correlated together to give accurate results constraining the paleodepositional environment and thermal maturity, as well as the quality of a source rock.

4.4.1. Pristane/phytane ratio (Pr/Ph)

The conditions of a source rock's depositional environment can be evaluated by the ratio of two alkanes: pristane (2, 6, 10, 14-tetramethyl pentadecane) and phytane (2, 6, 10, 14-tetramethyl hexadecane) [45,47]. The range of values for the Pr/Ph ratio indicates a variation in the redox conditions underwent by the source rock [48-49]. For the Hoiho Formation, the Pr/Ph ratio ranges from 3.9 to 7.0, reflecting the presence of mostly oxidizing terrestrial sediments (Table 3).

Table 3. Geochemical data, n-alkane and isoprenoid biomarker ratios

Well name	Hydrocarbons		n-alkane and isoprenoid biomarker ratios			
	TOC (wt. %)	EOM (ppm)	Pr/Ph	Pr/nC_{17}	Ph/nC_{18}	CPI
Hoiho-1C	61.23	3740.5	5.17	1.93	0.50	1.16
Kawau-1A	51.18	5936.3	3.93	0.48	0.13	1.01
	77.03	7407.7	6.00	1.29	0.21	1.03
	79.80	7463	7.15	1.35	0.19	0.98

Well name	Steranes				
	Regular steranes				
	C_{27}	C_{28}	C_{29}	$C_{27}/(C_{27}+C_{29})$	$C_{29}/(C_{29}+C_{27})$
Hoiho-1C	4.41	8.64	87.0	0.47	0.53
Kawau-1A	7.16	19.4	73.5	0.62	0.38
	0	21.5	78.5	0.60	0.40
	6.18	20.6	73.2	0.60	0.40

Key to biomarker abbreviation: ***Pr-*** *2,6,10,14-tetramethyl pentadecane;* ***Ph*** *-2,6,10,14-tetramethyl hexadecane;* ***IP*** *-$C_{20}H_{36}$;* ***dH*** *-18β-de-E-hopane*

4.4.2. Isoprenoid/n-alkanes ratio

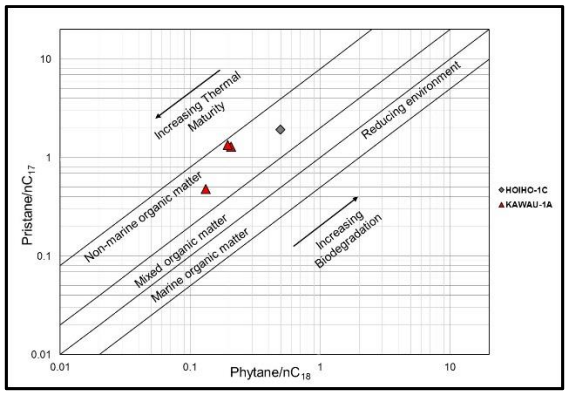

Figure 14. Graph of pristane/nC_{17} ratio versus phytane/ nC_{18} ratio calculated from gas chromatograms of maltene fraction of the Hoiho Formation (*adapted from Peters et al., 2005*)

The isoprenoids/n-alkanes ratios used in this study are the Pr/nC_{17} and Ph/nC_{18} ratios. These two parameters can indicate the biodegradation, maturation, and diagenetic state of a source rock. A correlation of these two ratios, as shown in Figure 14, indicates that the Hoiho Formation is dominantly made up of non-marine oxidizing organic matter. This agrees with the previously mentioned Pr/Ph ratio in 4.4.1.

4.4.3. Concentration of sterane biomarkers

The regular sterane biomarkers used for this study are C_{27}, C_{28} and C_{29}. Together, these steranes can indicate the origin of the organic matter making up the hydrocarbon. High concentrations of C_{27} sterane signify a marine origin for the organic matter. A dominance of C_{28} is caused by high levels of lacustrine algae and C_{29} dominance indicates a terrestrial origin. Volkman [50] stated that relying on steranes concentration to investigate the origin of organic matter is not always reliable. C_{29} sterane, which is originally thought to be derived from vascular plants, can also be found in sediments generated from a marine environment. A combination of results from other biomarkers derived from higher plants is therefore necessary to have a comprehensive understanding of the source of organic matter, especially from coals.

A ternary diagram, shown in Figure 15, has been constructed using C_{27}, C_{28} and C_{29} steranes to study the origin of organic matter (adapted after Huang and Meinschein [51]). Figure 15 shows that the organic matter of the Hoiho Formation is primarily terrestrial due to the dominance of the C_{29} sterane.

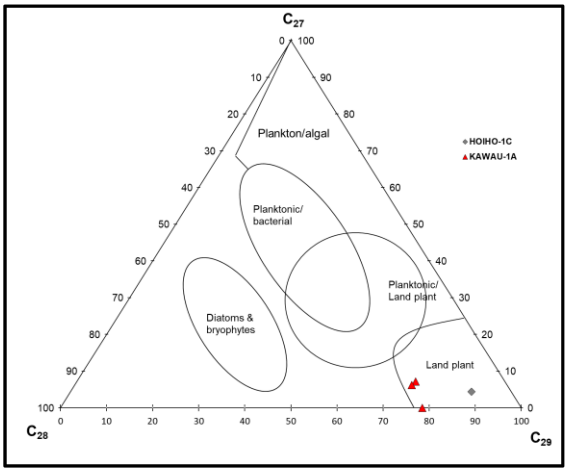

Figure 15. Ternary diagram of regular steranes for the Hoiho Formation (*adapted from Huang and Meinschein, 1979)*

4.4.4. Ratio of sterane and Pr/Ph

Conditions of the paleodepositional environment of the source rock were evaluated using a graph of $C_{27}/(C_{27}+C_{29})$ sterane versus Pr/Ph. Figure 16 indicates that the organic matter was deposited in a terrestrial and oxic environment.

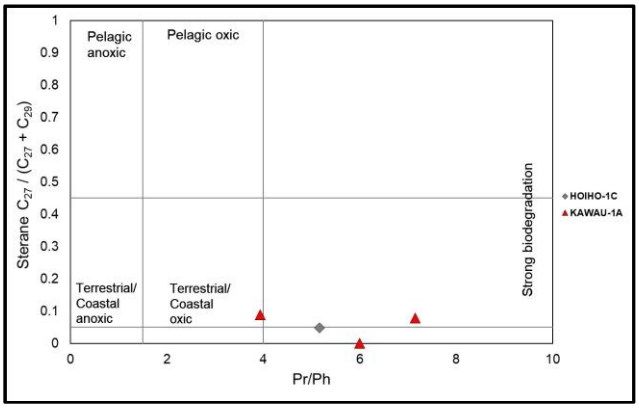

Figure 16. Cross-plots of C_{27} / (C_{27} + C_{29}) versus pristane/phytane ratio for the Hoiho Formation (*adapted from Hossain et al., 2009*)

4.4.5. Carbon Preference Index (CPI)

The Carbon Preference Index (CPI) of organic matter is defined as the ratio between the sum of odd-numbered carbon alkanes to the sum of even-numbered carbon alkanes. This parameter gives an indication of the state of a source rock's thermal maturity and the source of the organic matter [19]. A thermally immature source rock is indicated by CPI values that are significantly high or containing values that are less than 1.0 [47]. In this study, samples from the Hoiho Formation contain CPI values ranging from 1.0 to 1.2, indicating the organic matter of the Hoiho Formation is thermally mature and originates from a terrestrial source, which is in good agreement with figure 14 (Table 3).

4.4.6. Total organic carbon content (TOC) versus extractable organic matter (EOM)

Extractable organic matter derived from biomarkers can be used to assess the quality of source rock. In the cross-plot of total organic carbon (TOC) versus extractable organic matter (EOM), as shown in Figure 17, it is evident that the Hoiho source rock is of excellent quality and confirms the geochemical results as shown in Figures 4–5.

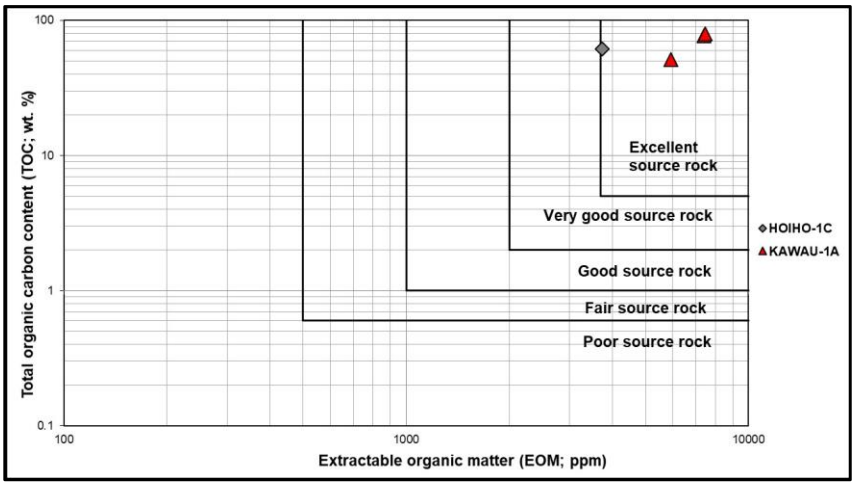

Figure 17. A cross-plot of TOC versus EOM to demonstrate the source rock quality

4.5. Burial history and Basin modelling

4.5.1. Subsidence and burial history

Through one-dimensional basin modelling using PetroMod software, several important factors can be assessed for the Hoiho source rock, including the burial history, sedimentation rate, thermal maturity history, maturation of source rock, and timing, as well as exact depth of hydrocarbon generation.

A total of eight formations are encountered in Kawau-1A well. The metamorphic basement is overlain by 442.5 m of the Late Cretaceous Hoiho Formation, which was deposited from 100.2 Ma for a duration of 13.7 Ma. Overlying this formation is the Kawau Sandstone, which was deposited from 86.5 Ma to 84.0 Ma, and serves as the reservoir for the underlying Hoiho Formation. Deposition of the Wickliffe Formation then follows for a duration of 18.5 Ma, producing a 955 m thick of sandy shale. The Waipawa Black Shale was deposited for a relatively short time, generating a thickness of 49 m. The Laing Formation is dominantly shale and was deposited from 55.8 Ma to 53.3 Ma to produce a layer of 157 m thick. The Tucker Cove Formation that lies above the Laing Formation consists primarily of shaley limestone. It has a present thickness 513 m and was deposited from 53.3 Ma to 34.5 Ma. Following the deposition of Tucker Cove Formation is the deposition of the Penrod Formation that has a duration of 18.6 Ma. From 15.9 Ma to the present, recent sediments are still being deposited

with shale as the main lithology (Fig. 18). Summary of the stratigraphic sequence for Kawau-1A well is found in Table 4.

Table 4. Input parameters for 1-D modelling of Well Kawau-1A

Formation name	Age (Ma)	Top (metres)	Bottom (metres)	Thickness (metres)	Lithology	Petroleum System Elements
Recent sediments	0-15.9	0	1100	1100	Shale	Overburden rock
Penrod Formation	15.9-34.5	1100	1550	450	Limestone	Overburden rock
Tucker Cove Formation	34.5-53.3	1550	2063	513	Shaly limestone	Overburden rock
Laing Formation	53.3-55.8	2063	2220	157	Shale	Overburden rock
Waipawa Black Shale	55.8-65.5	2220	2269	49	Shale	Overburden rock
Wickliffe Formation	65.5-84.0	2269	3224	955	Sandy shale	Seal rock
Kawau Sandstone	84.0-86.5	3224	3259.5	35.5	Sandy	Reservoir rock
Hoiho Formation	86.5-100.2	3259.5	3702	442.5	Shaly coal	Source rock

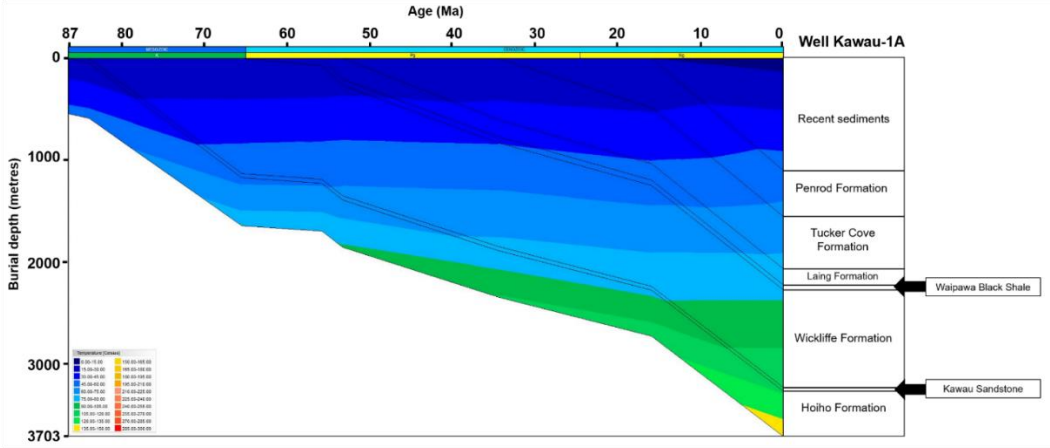

Figure 18. Burial history with temperature variations for Well Kawau-1A

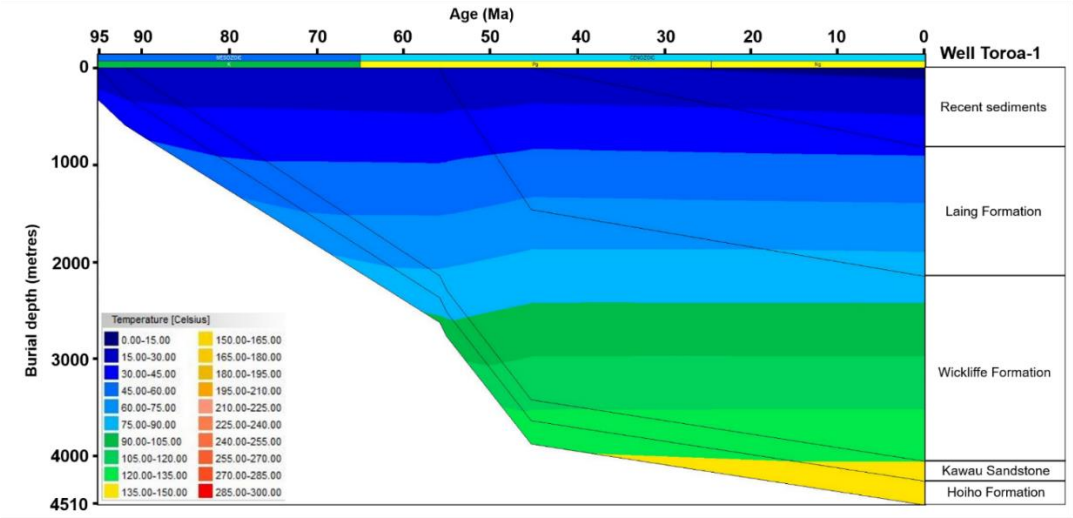

Figure 19. Burial history with temperature variations for Well Toroa-1

In the Toroa-1 well, the Late Cretaceous Hoiho Formation was deposited on top of the metamorphic basement from 100.2 Ma for a duration of 5 Ma. Overlying the Hoiho Formation is the Kawau Sandstone, which was deposited from 95.2 Ma to 92.1 Ma. Deposition of sandstone belonging to the Wickliffe Formation then occurred for 37.1 Ma, overlying the Kawau Sandstone. The Eocene Waipawa Black Shale is deposited afterwards with a thickness of 40 m from 55 Ma to 55.8 Ma. From 55.8 Ma to 45.3 Ma, the shale was further overlain by

the deposition of the Laing Formation, for which shale and sandstone are the main lithology. Following this is the deposition of recent sediments from 45.3 Ma to the present (Fig. 19). Table 5 indicates the succession of formation in Toroa-1 well.

Table 5. Input parameters for 1-D modelling of Well Toroa-1

Formation name	Age (Ma)	Top (metres)	Bottom (metres)	Thickness (metres)	Lithology	Petroleum System Elements
Recent sediments	0-45.3	0	823	823	Shale	Overburden rock
Laing Formation	45.3-55.0	823	2155	1332	Shale and Sandstone	Overburden rock
Waipawa Black Shale	55.0-55.8	2155	2195	40	Shale	Seal rock
Wickliffe Formation	55.8-92.1	2195	4100	1905	Sandstone	Reservoir rock
Kawau Sandstone	92.1-95.2	4100	4310	210	Sandstone	Reservoir rock
Hoiho Formation	95.2-100.2	4310	4551.5	241.5	Sandy coal	Source rock

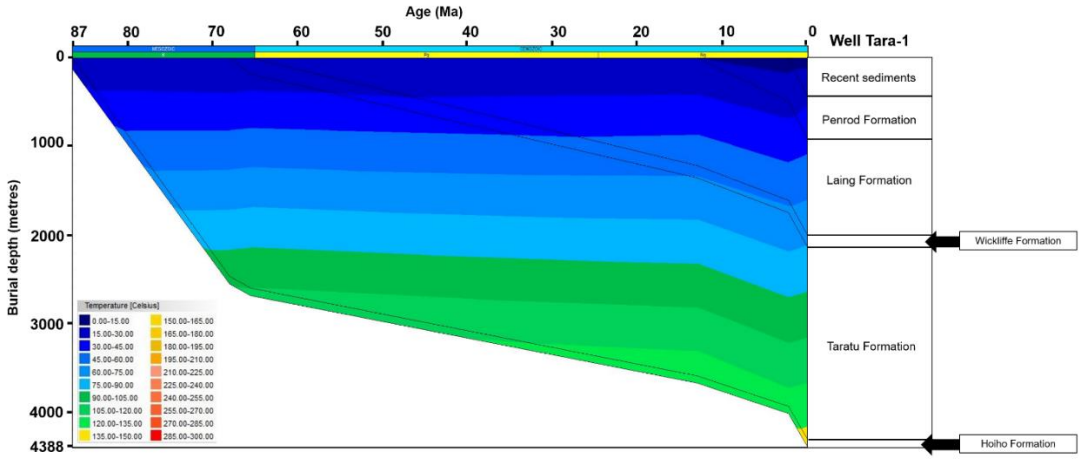

Figure 20. Burial history with temperature variations of Well Tara-1

The metamorphic basement of Tara-1 well is overlain by the Hoiho Formation which was deposited from 89.1 Ma to 86.5 Ma. Following this is the deposition of the Taratu Formation, which distinguishes Tara-1 well from the other two wells. With a thickness of 2165 m, the Paleocene and Late Cretaceous Taratu Formation was deposited from 86.5 Ma to 68 Ma. Overlying this is the sandy shale Wickliffe Formation that was deposited for a duration of 2.5 Ma. Deposition of Laing Formation then follows, from 65.5 Ma to 12.98 Ma to produce a 1086 m thick of sand and shale layer. Overlying the Laing Formation is the Penrod Formation, which was deposited 12.98 Ma to 2.2 Ma, with limestone as the main lithology. Recent sediments are then deposited from 2.2 Ma to the present (Fig. 20). Stratigraphy in Tara-1 well can be summarized in Table 6.

Table 6. Input parameters for 1-D modelling of Well Tara-1

Formation name	Age (Ma)	Top (metres)	Bottom (metres)	Thickness (metres)	Lithology	Petroleum System Elements
Recent sediments	0-2.2	0	442	442	Shale	Overburden rock
Penrod Formation	2.2-12.98	442	920	478	Limestone	Overburden rock
Laing Formation	12.98-65.5	920	2006	1086	Sandstone and shale	Overburden rock
Wickliffe Formation	65.5-68.0	2006	2139	133	Sandy shale	Seal rock
Taratu Formation	68.0-86.5	2139	4304	2165	Shaly sand	Reservoir rock
Hoiho Formation	86.5-89.1	4304	4387	83	Sandy coal	Source rock

4.5.2. Data calibration and thermal history

In the Great South Basin, heat flow is found to be more than 80 mW/m^2 [52] and is relatively higher than other basins, such as the Taranaki Basin, which has a heat flow ranging from less

than 50 mW/m^2 to more than 70 mW/m^2. The elevated heat flow found in the Great South Basin will influence the maturity of source rocks and hydrocarbon generation. According to Uruski and Ilg [13], there is an elevated heat flow value of approximately 90 mW/m^2 due to a heat flow anomaly towards the area around Dunedin.

Borehole temperature (BHT) values recorded do not reflect accurate formation values as the readings are taken before temperature equilibrium between the drilling mud and the formation is reached. For this reason, raw BHT readings are considerably lower than actual formation temperatures and must be corrected. In this study, corrections of BHT are performed based on studies by Waples and Ramly [25], Waples and Ramly [26], Peters and Nelson [27] and Bullard [28]. Corrected temperatures are compared with modelled temperature values for calibration purposes, and a best fit between those two values indicates excellent data quality. Similarly, calibration was undertaken between measured vitrinite reflectance and calculated values based on the EASY%R$_o$ model [29] are undertaken.

For Kawau-1A, Toroa-1 and Tara-1 wells, calibration of temperature and vitrinite reflectance at all depths display a generally good fit with each other. A minor offset in temperature calibration is detected in Kawau-1A well (Fig. 21) but there is an excellent fit for modelled and measured vitrinite reflectance values (Fig. 22). In Figures 23 to 25, an excellent fit for measured and modelled temperature as well as vitrinite reflectance values are detected for both Toroa-1 and Tara-1 wells.

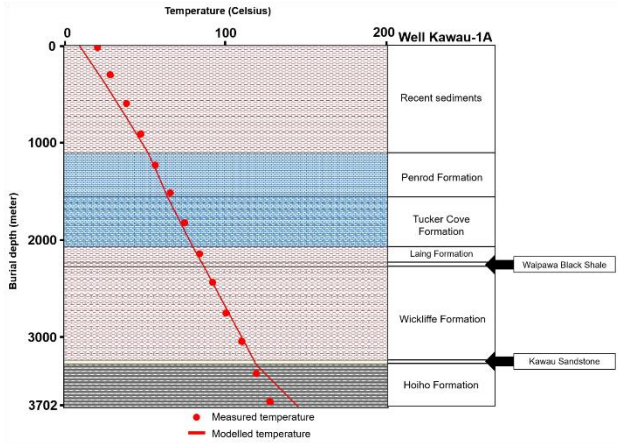

Figure 21. Calibration of measured and modelled temperature for Well Kawau-1A

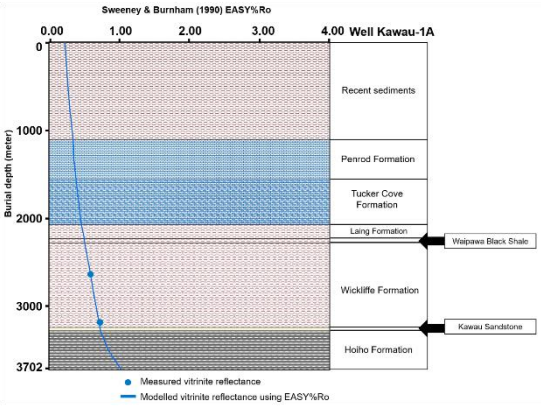

Figure 22. Calibration of measured and modelled vitrinite reflectance values for Well Kawau-1A

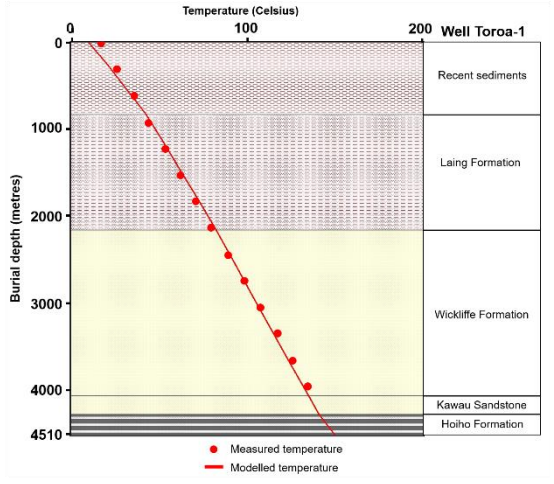

Figure 23. Calibration of measured and modelled temperature for Well Toroa-1

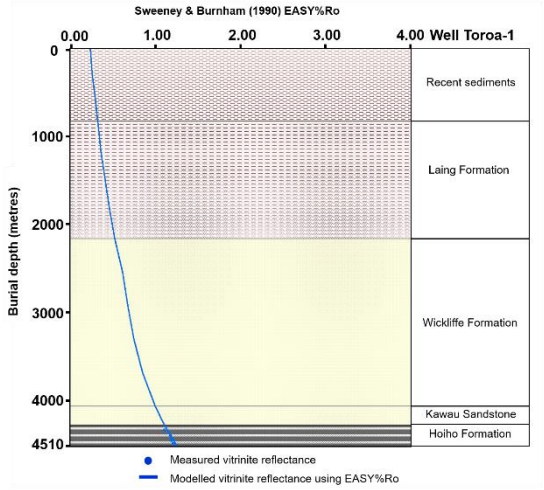

Figure 24. Calibration of measured and modelled vitrinite reflectance values for Well Toroa-1

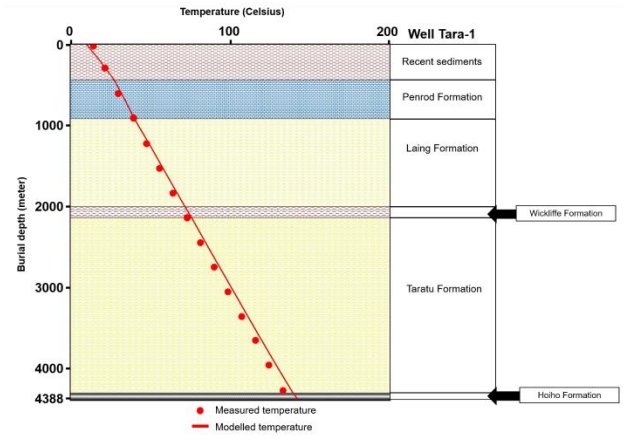

Figure 25. Calibration of measured and modelled temperature for Well Tara-1

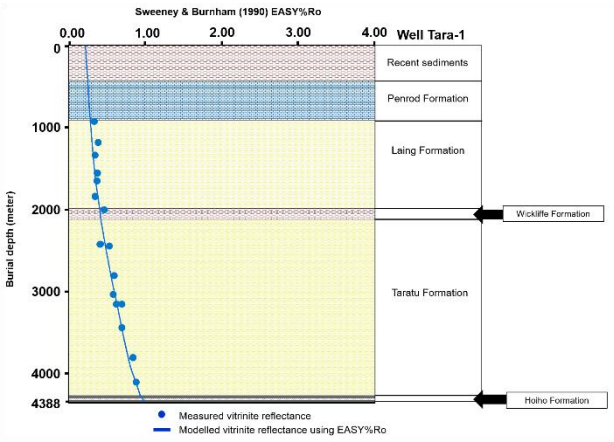

Figure 26. Calibration of measured and modelled tem-perature for Well Toroa-1

4.5.3. Timing of hydrocarbon generation and expulsion in the Hoiho Formation

1-D modelling from all wells permits the identification of the exact timing and depth of hydrocarbon generation and expulsion for the Hoiho source rocks. This was done based on formation temperature and maturation history [44]. Figures 26 to 31 show the hydrocarbon generation models for Kawau-1A, Toroa-1 and Tara-1 wells, with reference to the study by Burnham [53], together with their respective hydrocarbon multi-component ratio model.

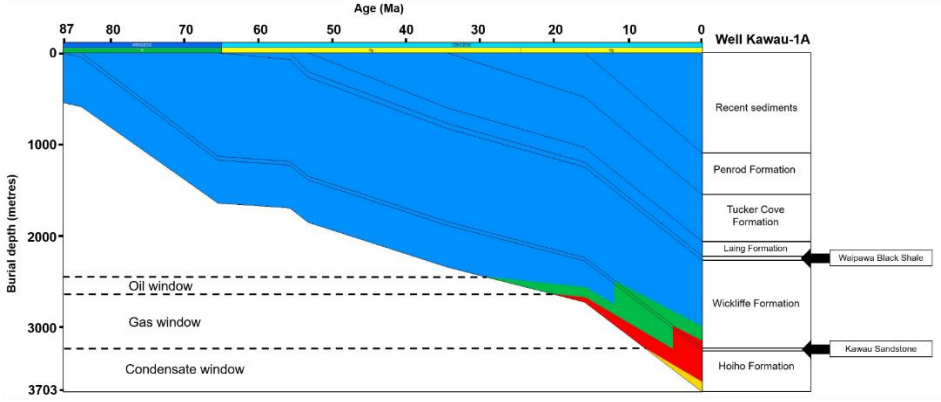

Figure 27. Hydrocarbon generation model indicating oil, gas and overmaturation windows for Well Kawau-1A

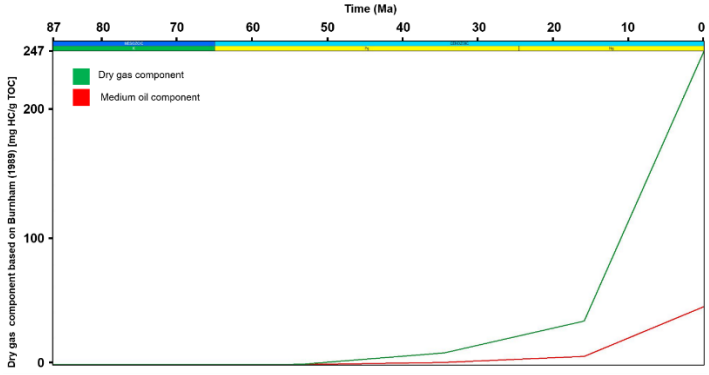

Figure 28. Hydrocarbon multi-component ratios for Well Kawau-1A

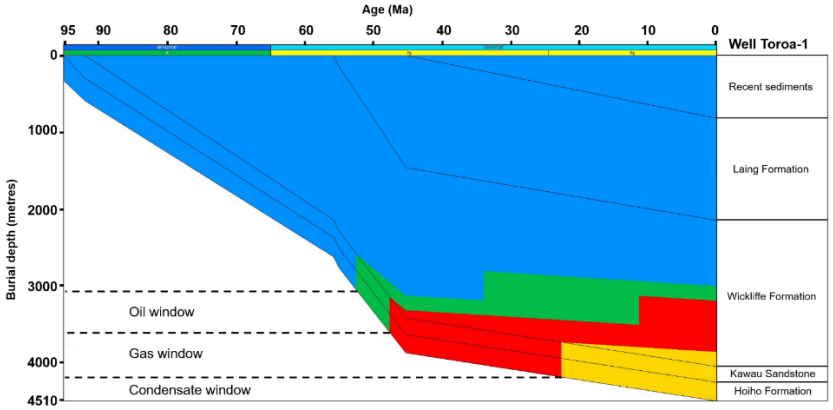

Figure 29. Hydrocarbon generation model indicating oil, gas and overmaturation windows for Well Toroa-1

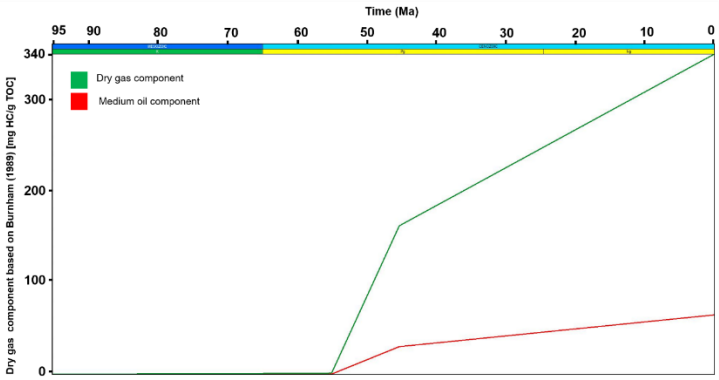

Figure 30. Hydrocarbon multi-component for Well Toroa-1

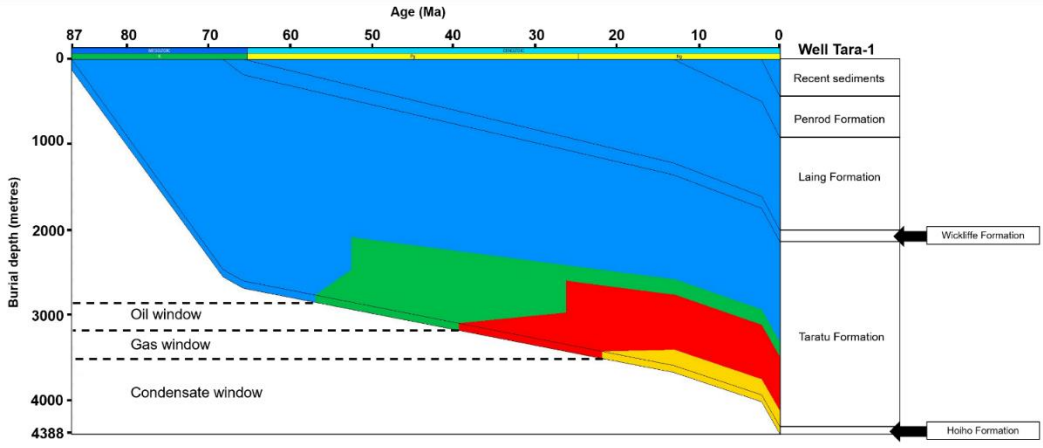

Figure 31. Hydrocarbon generation model indicating oil, gas and overmaturation windows for Well Tara-1

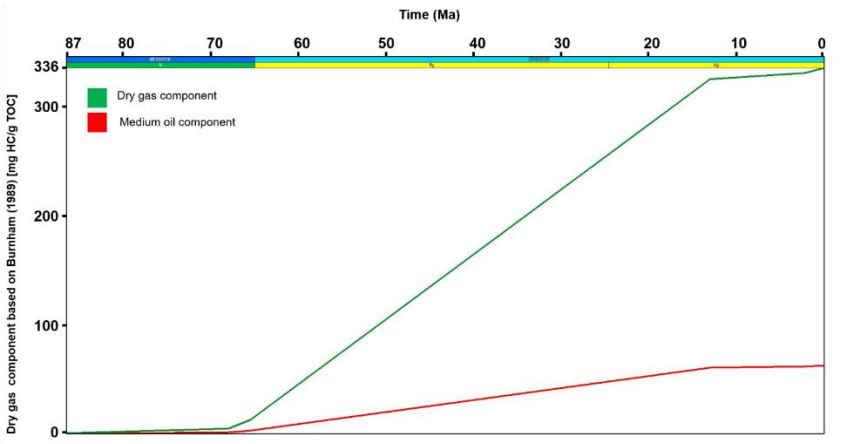

Figure 32. Hydrocarbon multi-component for Well Tara-1

In Kawau-1A, the top of oil window of the Hoiho Formation was achieved 29 Ma ago at a depth of 2448 m and in 20 Ma, the hydrocarbon matures to gas at 2634 m depth (Fig. 26). Over maturity for the Hoiho Formation in this well was reached at 3227 m depth in 8 Ma. At the present, oil and gas is still being generated in Kawau-1A well as shown in Figure 27.

The oil generation window for the Hoiho source rock began at 53 Ma at a depth of 3056 m for Toroa-1. At 48 Ma, the top of gas window was reached at a depth of 3601 m. In this well, over maturity of organic matter was attained at 23 Ma ago at a depth of 4206 m (Fig. 28). At the present, 340 mg HC/g TOC of dry gas has been produced and the generation of liquid hydrocarbon has not yet reached its peak (Fig. 29).

At a depth of 2853 m, the oil generation window for the Hoiho Formation was reached in 57 Ma for Tara-1 well. The top of gas window for this well is reached at a depth of 3183 m in 39 Ma and overmaturity is reached at 3508 m in 22 Ma (Fig. 30). For Tara-1 well, there is a rapid generation of gas for a duration of 55 Ma with a concentration of 325 mg HC/g TOC (Fig. 31).

5. Conclusions

This study demonstrates the excellent potential of the Hoiho Formation in the Great South Basin of New Zealand as a promising source rock that may generate excellent hydrocarbon quality and quantity. In pyrolysis performed on rock samples belonging to four wells, high TOC with moderate HI readings are produced, indicating the presence of kerogen types II-III and kerogen type III. Studying thermal maturity in terms of T_{max}, vitrinite reflectance and other pyrolysis results indicates that the source rock is generally thermally mature but can be immature when drilled at a relatively shallower depths of approximately less than 2500 m. At greater depths of more than 4400 m, the organic matter is thermally over-mature. The results also show that maturity of the Hoiho source rock is higher at only three out of four studied wells due to the positions of these wells in the Great South Basins. One-dimensional basin modelling of the Hoiho source rock for Kawau-1A, Toroa-1 and Tara-1 provide an understanding of the burial and thermal maturity history of the formation. The results show that a best-fit between measured and calculated/modelled values for vitrinite reflectance and borehole temperatures in both wells. The top of oil window was reached earlier in Kawau-1A (approximately 29 Ma) while Toroa-1 and Tara-1 began to generate liquid hydrocarbon at approximately 53 Ma and 57 Ma respectively. Biomarker parameters used together with their derivations all confirm that the paleodepositional environment of the Hoiho source rock was originally non-marine and possibly located in a coastal swamp environment where marine influence is present.

Acknowledgement

The authors would like to express their gratitude to New Zealand Petroleum and Minerals, Ministry of Business, Innovation & Employment and GNS Science for providing the data for this study. Thanks and appreciations are also extended to University Brunei Darussalam for providing all facilities and support to complete this research.

References

[1] Schiøler P, Rogers K, Sykes R, Hollis CJ, Ilg B, Meadows D, Roncaglia L and Uruski C. Palynofacies, organic geochemistry and depositional environment of the Tartan Formation (Late Paleocene), a potential source rock in the Great South Basin, New Zealand. Mar. Pet. Geol. 2009; 27(2): 351-369.
[2] Evans PR. Petroleum potential of New Zealand. J. Pet. Geol. 1982; 5(1) 89-96.
[3] Beggs JM. Depositional and tectonic history of the Great South Basin. South Pacific sedimentary basins. Sedimentary basins of the World. 1993; (2) 93-107.
[4] Cook RA, Sutherland R and Zhu H. Cretaceous-Cenozoic Geology and Petroleum Systems of the Great South Basin, New Zealand. Institute of Geological & Nuclear Sciences. 1999; 20.
[5] Lipski PS. Evidence for an oil play fairway on the inner shelf of the Great South Basin, New Zealand. New Zealand Petroleum Conference Proceedings. 2004; 7-10.
[6] Kuehnert HA. Source rock potential of Hunt's Kawau-1A, New Zealand. Petroleum report. 1977; 737.
[7] Gibbons MJ and Jackson RG. A geochemical review of the Great South Basin (incorporating previously unreported data for Kawau-1 and Toroa-1). Petroleum report. 1980; 902.
[8] Anderton PW, Holloway NH, Engstrom JC, Ahmad HM and Chong B. Evaluation of the geology and hydrocarbon potential of the Great South and Campbell Basins. Petroleum report. 1982; 828.
[9] Killops SD, Cook RA, Sykes R and Boudou JP. Petroleum potential and oil-source correlation in the Great South and Canterbury Basins. N. Z. J. Geol. Geophys. 1997; 40: 405-423.
[10] New Zealand Petroleum and Minerals. New Zealand Petroleum Basins. Ministry of Business, Innovation and Employment. New Zealand: New Zealand Petroleum and Minerals, New Zealand. 2014.
[11] Uruski CI and Baillie P. Petroleum potential of New Zealand's deepwater basins. PESA Eastern Australasia Basins Symposium. 2001; 151-158.
[12] Pearson AR. The Great South Basin–Antrim International's Exploration Strategy. Proceedings of the 1998 New Zealand Petroleum Conference. Ministry of Commerce, Wellington. 1998; 123-139.
[13] Uruski CI and Ilg B. Preliminary Interpretation and Structural Modelling of DUN06 Seismic Reflection Data from Great South Basin, Offshore New Zealand, Ministry of Economic Development New Zealand Unpublished Petroleum Report PR3450. 2006.
[14] McMillan SG and Wilson GJ. Allostratigraphy of coastal south and east Otago: a stratigraphic framework for interpretation of the Great South Basin, New Zealand. N. Z. J. Geol. Geophys. 1997; 40(1): 91-107.
[15] Constable RM, Langdale S and Allan TMH. Development of a sequence stratigraphic framework in the Great South Basin. Advantage NZ: 2013 Petroleum Conference, Wellington. 2013; 1-21.
[16] Laird MG and Bradshaw JD. The break-up of a long-term relationship: the Cretaceous separation of New Zealand from Gondwana. Gondwana Res. 2004; 7 (1): 273-286.
[17] Laird M. Mid and early Late Cretaceous break-up basins of the South Island, New Zealand. In Geological Society of Australia Abstracts. Geological Society of Australia. 1996; 43: 329-336.
[18] King PR. Tectonic reconstructions of New Zealand: 40 Ma to the present. N. Z. J. Geol. Geophys. 2000; 43(4): 611-638.
[19] Tissot BP and Welte DH. Petroleum Formation and Occurrence: A New Approach to Oil and Gas Exploration. Berlin: Springer-Verlag. 1978; 538.
[20] Peters KE. Guidelines for evaluating petroleum source rock using programmed pyrolysis. AAPG Bull. 1986; 70(3): 318-329.
[21] Espitalié J, Madec M, Tissot, B., Mennig JJ and Leplat P. Source rock characterization method for petroleum exploration. Offshore Technology Conference. 1977.
[22] Rodriguez ND and Philp RP. Source rock facies distribution predicted from oil geochemistry in the Central Sumatra Basin, Indonesia. AAPG Bull. 2015; 99(11): 2005-2022.
[23] Abdullah WH, Togunwa OS, Makeen YM, Hakimi MH, Mustapha KA, Baharuddin MH, Sia S-G and Tongkul F. Hydrocarbon source potential of Eocene-Miocene sequence of Western Sabah, Malaysia. Mar. Pet. Geol. 2017; 83: 345-361.

[24] Ayinla HA, Abdullah WH, Makeen YM, Abubakar MB, Jauro A, Yandoka BMS, Mustapha KA and Abidin NSZ. Source rock characteristics, depositional setting and hydrocarbon generation potential of Cretaceous coals and organic rich mudstones from Gombe Formation, Gongola Sub-basin, Northern Benue Trough, NE Nigeria. International Journal of Coal Geology 2017; 173: 212-226.
[25] Waples DW and Ramly M. A simple statistical method for correcting and standardizing heat flows and subsurface temperatures derived from log and test data. Bulletin of the Geological Society of Malaysia, Special Publication. 1994; 37: 253-267.
[26] Waples DW and Ramly M. A statistical method for correcting log-derived temperatures. Pet. Geosci. 2001; 7(3): 231-240.
[27] Criteria to determine borehole formation temperatures for calibration of basin and petroleum system models. Thermal history analysis of sedimentary basin: Methods and applications: SEPM Special Publication. 2013; 103: 5-16.
[28] Bullard EC. The time necessary for a bore hole to attain temperature equilibrium. Geophys. J. Int. 1947; 5(5): 127-130.
[29] Sweeney JJ and Burnham AK. Evaluation of a simple model of vitrinite reflectance based on chemical kinetics (1). AAPG Bull. 1990; 74(10): 1559-1570.
[30] Shalaby MR, Hakimi MH and Abdullah WH. Geochemical characteristics and hydrocarbon generation modeling of the Jurassic source rocks in the Shoushan Basin, north Western Desert, Egypt. Mar. Pet. Geol. 2011; 28(9): 1611-1624.
[31] Shalaby MR, Hakimi MH and Abdullah WH. Modeling of gas generation from the Alam El-Bueib formation in the Shoushan Basin, northern Western Desert of Egypt. Int. J. Earth Sci. 2012a; 102(1): 319-332.
[32] Shalaby MR, Hakimi MH and Abdullah WH. Organic geochemical characteristics and interpreted depositional environment of the Khatatba Formation, northern Western Desert, Egypt. AAPG Bull. 2012b; 96: 2019–2036.
[33] Shalaby MR, Hakimi MH and Abdullah WH. Geochemical characterization of solid bitumen (migrabitumen) in the Jurassic sandstone reservoir of the Tut Field, Shushan Basin, northern Western Desert of Egypt. International Journal of Coal Geology. 2012c; 100: 26-39.
[34] El Nady MM, Ramadan FS, Hammad MM and Lotfy NM. Evaluation of organic matters, hydrocarbon potential and thermal maturity of source rocks based on geochemical and statistical methods: Case study of source rocks in Ras Gharib oilfield, central Gulf of Suez, Egypt. Egypt. J. Pet. 2015; 24(2): 203-211.
[35] Langford FF and Blanc-Valleron MM. Interpreting Rock-Eval pyrolysis data using graphs of pyrolizable hydrocarbons vs. total organic carbon (1). AAPG Bull. 1990; 74(6): 799-804.
[36] Espitalié J, Deroo G and Marquis F. Rock-Eval pyrolysis and its applications. Revue De L Institut Francais Du Petrole 1985; 40(5): 563-579.
[37] Waples DW. Geochemistry in petroleum exploration, D. Reidel Publishing Co.: Dordrecht-Boston-Lancaster, 1985; pp. 1-232.
[38] Peters KE and Cassa MR. Applied source-rock geochemistry, Magoon, L.B., Dow, W.G., Eds.; The Petroleum System—From Source to Trap. AAPG Mem. 1994; 60: 93–120.
[39] Espitalié J. Use of Tmax as a maturation index for different types of organic matter, Burrus, J., Ed.: Editions Technip Paris, 1986; pp. 475-496.
[40] Barker C. Pyrolysis techniques for source-rock evaluation. AAPG Bull. 1974; 58(11): 2349-2361.
[41] Mukhopadhyay PK. Vitrinite reflectance as a maturity parameter. 1994; 570: 1-24.
[42] Stach E, Mackowsky MT, Teichmüller M, Taylor GH, Chandra D and Teichmüller R. Stach's textbook of coal petrography. Borntraeger, Berlin. 1982; pp. 1-535.
[43] Price LC and Barker CE. Suppression of vitrinite reflectance in amorphous rich kerogen--a major unrecognized problem. J. Pet. Geol. 1985; 8(1): 59-84.
[44] Qadri ST, Shalaby MR, Islam MA and Hoon LL. Source rock characterization and hydrocarbon generation modeling of the Middle to Late Eocene Mangahewa Formation in Taranaki Basin, New Zealand. Arabian J. Geosci. 2016; 9(10): 559, 8-9.
[45] Moustafa YM and Morsi RE. Biomarkers. Chromatography and its Applications. InTech. 2012.
[46] Mobarakabad AF, Bechtel A, Gratzer R, Mohsenian E and Sachsenhofer RF. Geochemistry and origin of crude oils and condensates from the Central Persian Gulf, Offshore Iran. J. Pet. Geol. 2011; 34(3): 261-275.
[47] Peters K, Walters C and Moldowan J. The Biomarker Guide: Biomarkers and isotopes in petroleum systems and Earth history. Cambridge University press, New York. 2005; 2(2).

[48] Powell TG and McKirdy DM. Relationship between ratio of pristane to phytane, crude oil composition and geological environment in Australia. Nature. 1973; 243(124): 37-39.
[49] Didyk BM. Organic geochemical indicators of palaeoenvironmental conditions of sedimentation. Nature. 1978; 272: 216-222.
[50] Volkman JK. A review of sterol markers for marine and terrigenous organic matter. Org. Geochem. 1986; 9(2): 83-99.
[51] Huang WY and Meinschein WG. Sterols as ecological indicators. Geochim. Cosmochim. Acta 1979; 43(5): 739-745.
[52] Townend J. Heat flow through the west coast, South Island, New Zealand. N. Z. J. Geol. Geophys. 1999; 42(1): 21-31.
[53] Burnham AK. A simple kinetic model of petroleum formation and cracking. Lawrence Livermore National Lab, California; 1989.
[54] Fakhri M, Tabatabei H and Amiri A. Comparing the Potential of Hydrocarbon Generation of Kazhdomi and Pabdeh Formations in Bangestan Anticline (Zagros Basin) According To Rock-Eval Pyrolysis Data. J. Earth Sci. Clim. Change. 2013; 4(157).
[55] Hossain HZ, Sampei Y and Roser BP. Characterization of organic matter and depositional environment of Tertiary mudstones from the Sylhet Basin, Bangladesh. Org. Geochem. 2009; 40(7): 743-754.

To whom correspondence should be addressed: Liyana N. Osli, Department of Geology, Faculty of Science, Universiti Brunei Darussalam, Jalan Tungku Link, BE 1410, Brunei Darussalam, anadiah.osli@gmail.com